Supplementary Material

Influence of the oxidic support material on the platinum-catalyzed benzyl alcohol oxidation

Avela Kunene[†] and Eric van Steen[*]

Catalysis Institute, Department of Chemical Engineering, University of Cape Town, Private Bag X3, Rondebosch 7701, South Africa; † Present address: Helmholtz Zentrum Berlin für Materialien und Energie, Hahn-Meitner-Platz 1, 14109 Berlin, Germany
Email: eric.vansteen@uct.ac.za

Table of Contents

Determination of the contact angle using the Washburn method S2
NH_3-TPD-profiles S5
Pt-particle size distributions.....S6
Dispersion of catalysts in water/benzyl alcohol mixture S7
Reactor set-up and procedures.....S8
Benzyl alcohol conversion as a function of reaction time S9
Correlating the adsorption of water with the energy for the formation of a vacancy in the support materials.....S10

1. Determination of the contact angle using the Washburn method

The contact angle of water with each of the support materials was determined using the Washburn method.[S1,S2] Prior to the experiments, the samples were not heat treated, but stored in a desiccator to ensure reproducible state of the material. In this method, the mass change is followed as a function of time:

$$\frac{m^2}{t} = C_w \cdot \rho^2 \cdot \frac{\gamma}{\eta} \cdot \cos\theta$$

With m mass increase of the sample due to liquid uptake
t time taken for the liquid rise into capillary.
C_w capillary constant.
ρ density of liquid.
γ surface tension of liquid.
η viscosity of the liquid.
θ contact angle of the liquid on capillary walls.

The capillary constant was determined by n-hexane, assumed to be fully wetting. The linear dependence of square of the mass increase with time was used to determine the capillary constant (see Table S.1). The various support materials will have various capillary constants as to the packing of these materials in the capillary depends on the particle size and shape.

Table S1. Capillary constant for the different support materials

.	TiO_2(P25)	γ-Al_2O_3	CeO_2	MoO_3	γ-Fe_2O_3
C_W, 10^{-6} cm^5	2.14	2.35	0.79	1.06	1.81

The determination of the contact angle of water with the support is not straight forward as the slope of the curve of the mass increase squared as a function of time may change (see Fig. S1). The slope can be determined using an integral method (i.e. directly from the measured mass increase at a given time) or a differential method (i.e. by determining the slope as a moving average). These two methods do not yield the same result. The reported contact angle of the support was determined by determining the initial slope using the differential method.

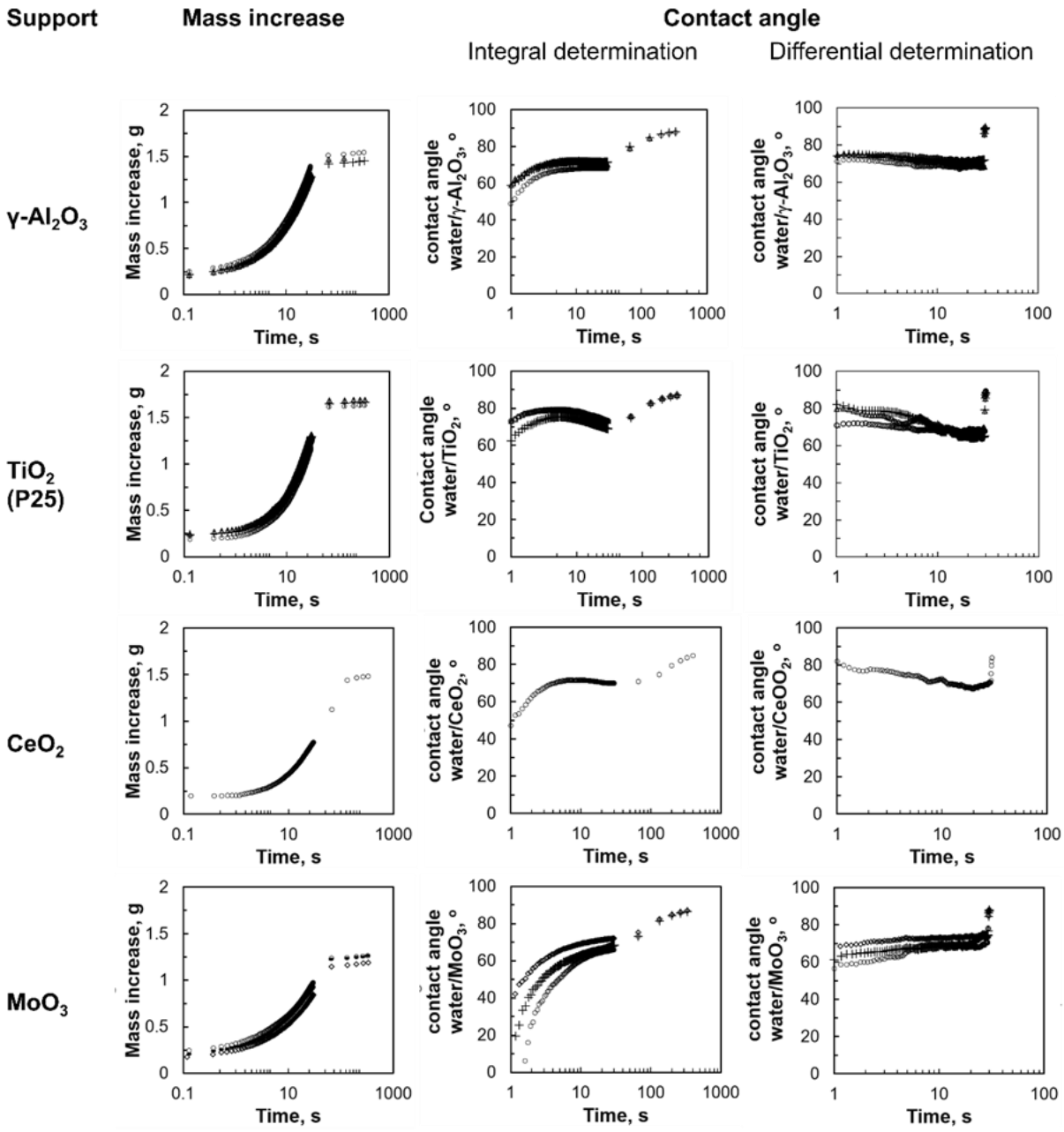

Figure S1. Mass uptake (on a logarithmic time scale) as a function of time and the determination of the contact angle of water using the Washburn method[S1,S2]

The measured contact angles are given in Table S.2. The main contribution to the variation in the determined contact angle is the variation in the packing (thus showing the influence of the packing on the capillary constant, which was assumed to be constant).

The measured contact angle of water with γ-Al_2O_3 is in reasonable agreement with the reported one of 68.4°,[S3] which was determined using the same method, but smaller than the contact angle measured using water droplets.[S4] The reported contact angle of water with TiO_2 (P25) was determined to be 80.5°, well within the range of the reported (large) variability of the contact angle of water on P25.[S5] The determined contact angle for ceria is in the expected range for the low Miller index surfaces of CeO_2.[S6] Molybdenum oxide[S7] and maghemite[S8] are

more hydrophilic, and a contact angle of water of 63.5° (MoO_3) and 65.3° (γ-Al_2O_3) were determined.

Table S2. Contact angles of water with the various support materials

.	γ-Al_2O_3	TiO_2(P25)	CeO_2	MoO_3	γ-Fe_2O_3
Contact angle, °	73.8 ± 1.4	80.4 ± 2.1	78.3 ± 1.9	63.5 ± 4.5	65.3
Heat of immersion, J/m^2	-0.106	-0.956	-2.875	58.9	-0.198

The contact angle measurements were complemented by heat of immersion measurements. The obtained values is a strong function of the level of hydration on the surface.[S9-S11] The heat of immersion of CeO_2 is rather high, which may be attributed to the change in the surface composition upon exposure to liquid water.[S7] The measured heat of immersion of MoO_3 in water shows that dissolution of molybdenum oxide has taken place.

2. NH_3-TPD-profiles

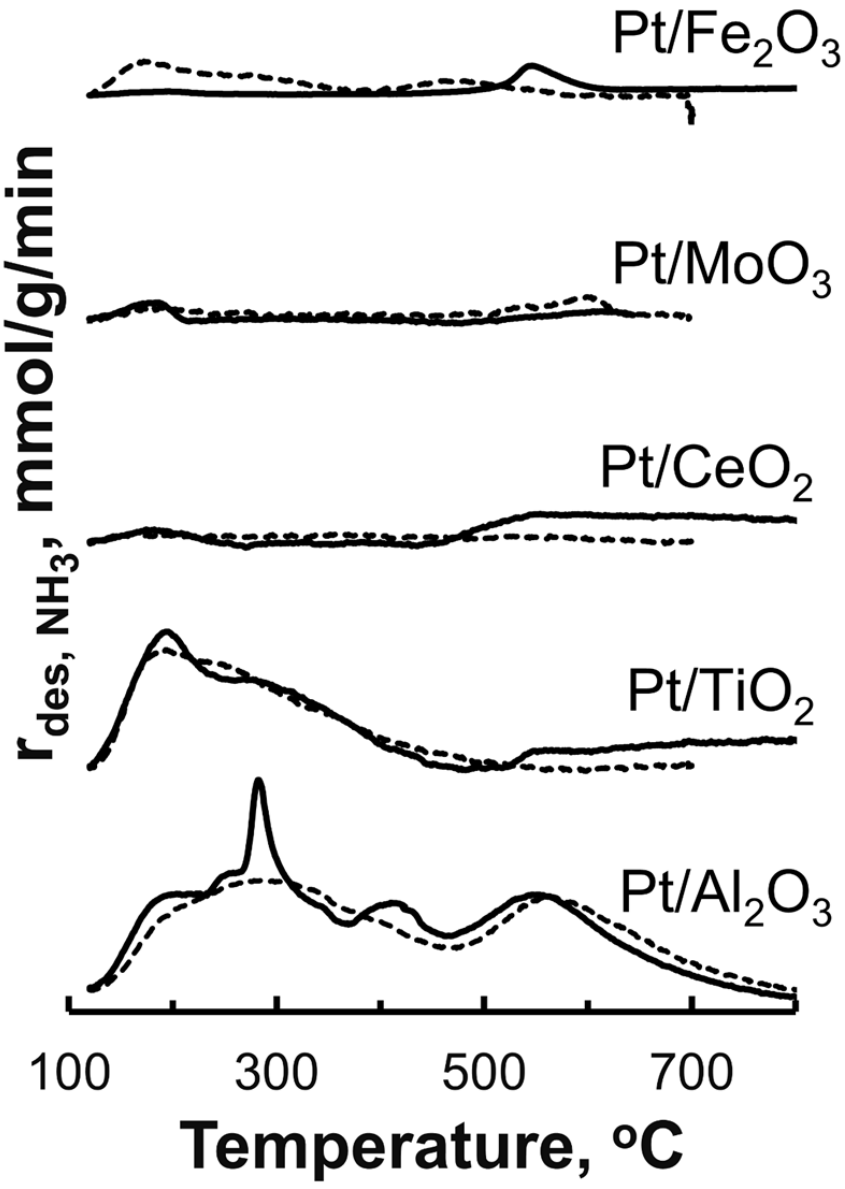

Figure S2. NH_3-TPD profiles of the supported catalysts (solid curves) and the support materials (dotted curves)

3. Pt-particle size distributions

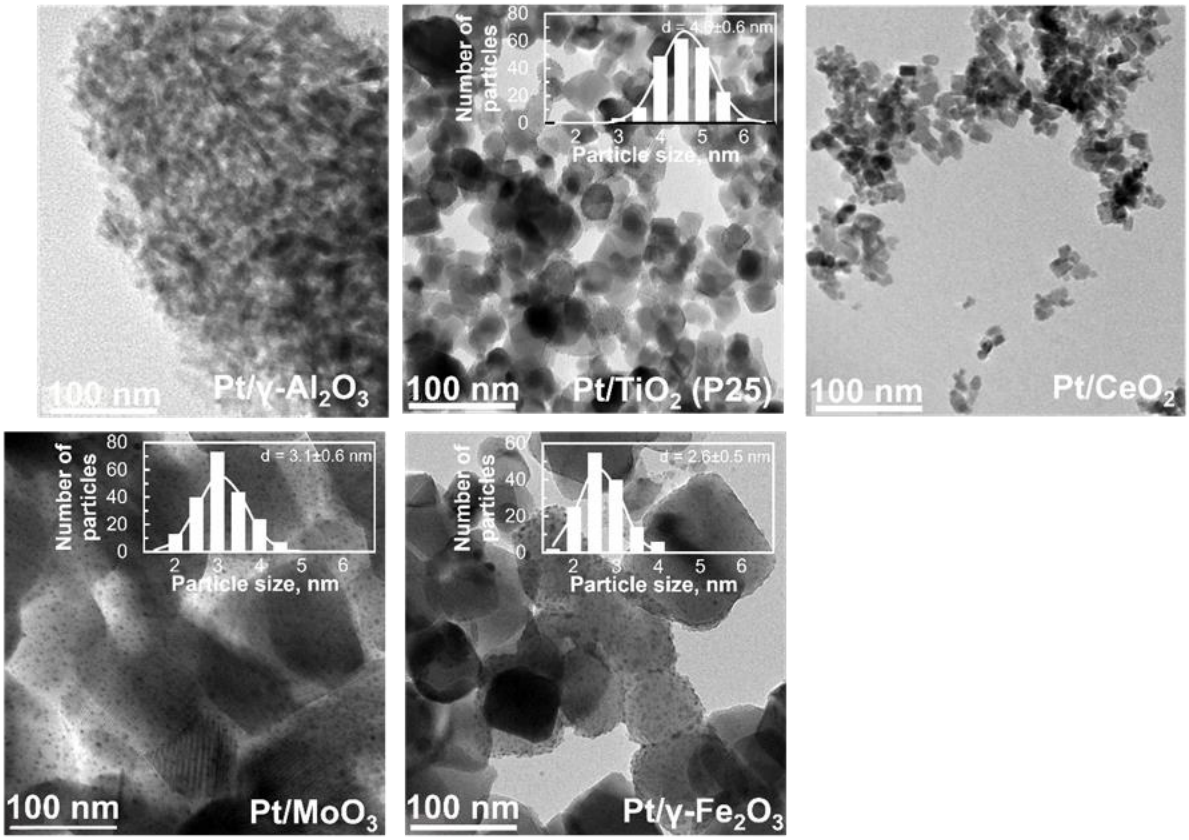

Figure S3. TEM-images of the catalysts and the obtained particle size distributions by counting at least 100 particles (curves in the particle size distribution represent the best fit Gaussian distribution).

4. Dispersion of catalysts in water/benzyl alcohol mixture

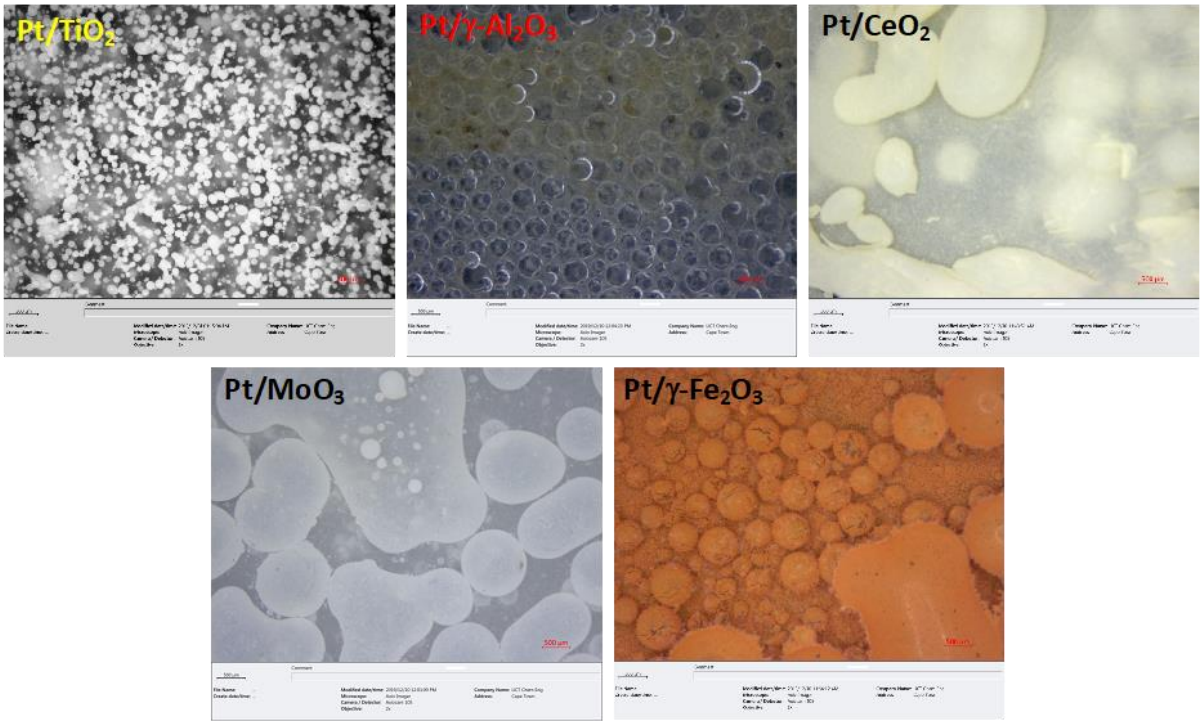

Figure S4. Micrographs of a platinum-based catalyst supported on various oxides suspended in an emulsion containing 93 mol-%H_2O and 7 mol-% benzyl alcohol.

5. Reactor set-up and procedures

The catalytic activity for the benzyl alcohol oxidation was tested in an autoclave (250 mL) filled initially 70 mL of liquid with an initial concentration of benzyl alcohol of 2.8 M in water and 0.5 g catalyst. The reaction is thus carried out in a bi-phasic liquid system. The mixture was intensively stirred (850 rpm) and brought to the reaction temperature (either 90°C) with a heating rate of 10°C/min. The aerobic oxidation was performed by sparging air through the solution (100 mL_n/min) keeping the total pressure above the reaction mixture at 5 bar (the effluent gas passed a condenser operating at -7°C with the liquid returning to the reaction vessel). Samples (0.1 mL) were withdrawn hourly from the reactor through a dip tube during the 5-hour run. The samples were homogenized using methanol and the organic products were separated using gas chromatography and analysed with an FID.

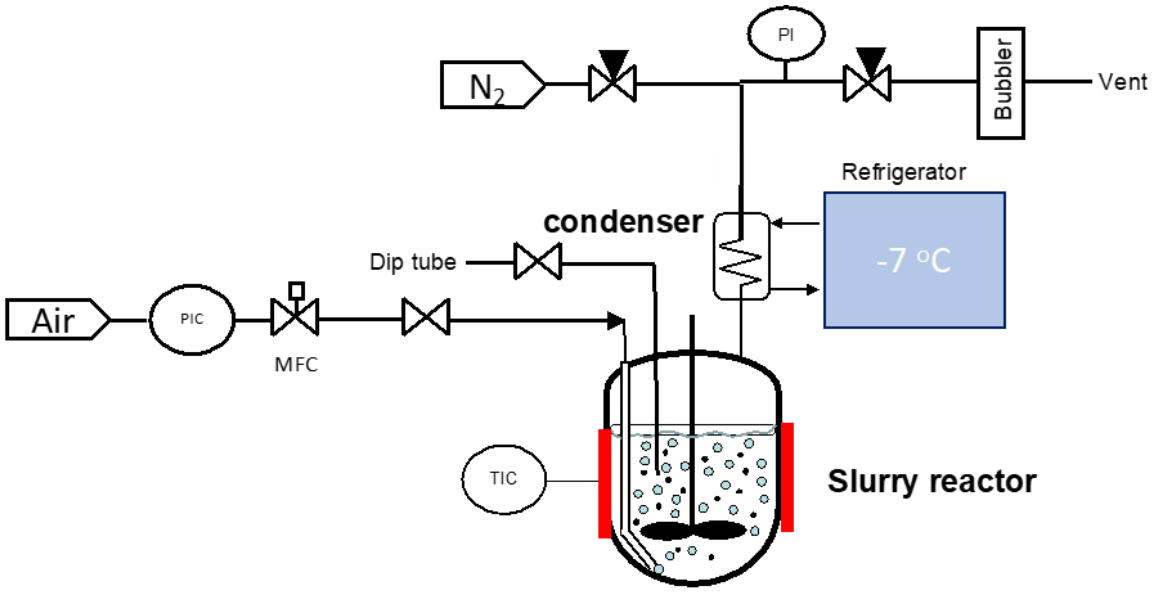

Figure S5. Semi-batch reactor schematic for alcohol oxidation reaction. PIC: pressure control valves; TIC: temperature controller, MFC: Mass Flow Controller, PI: pressure indicator and TI: temperature indicator.

A GC (Varian 3400) fitted with a flame ionization detector (FID) was used to analyse the organic compounds in the samples.

6. Benzyl alcohol conversion as a function of reaction time

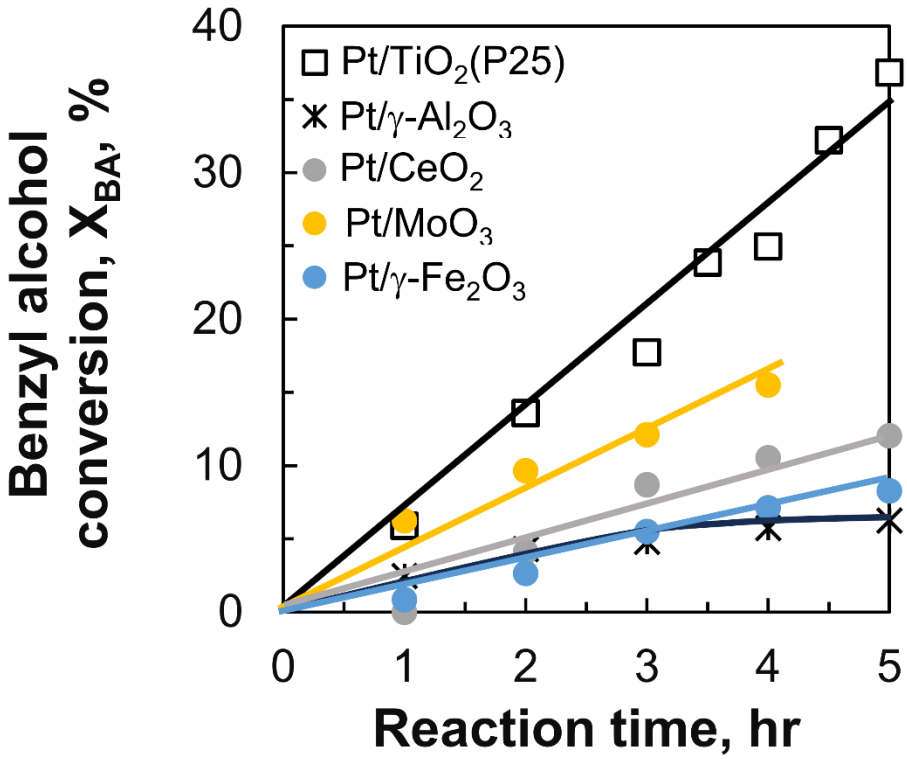

Figure S6. Benzyl alcohol conversion over Pt/TiO_2(P25), Pt/γ-Al_2O_3, Pt/CeO_2, Pt/MoO_3 and Pt/γ-Fe_2O_3 as a function of reaction time in pure benzyl alcohol (left) and in a benzyl alcohol/water mixture containing 7 mol-% benzyl alcohol (right). Conditions: T = 90°C, p = 5 bar, air flow rate = 100 mL_n/min, $m_{catalyst}$ = 0.5 g, V_{liquid} = 70 mL).

7. Correlating the adsorption of water with the energy for the formation of a vacancy in the support materials

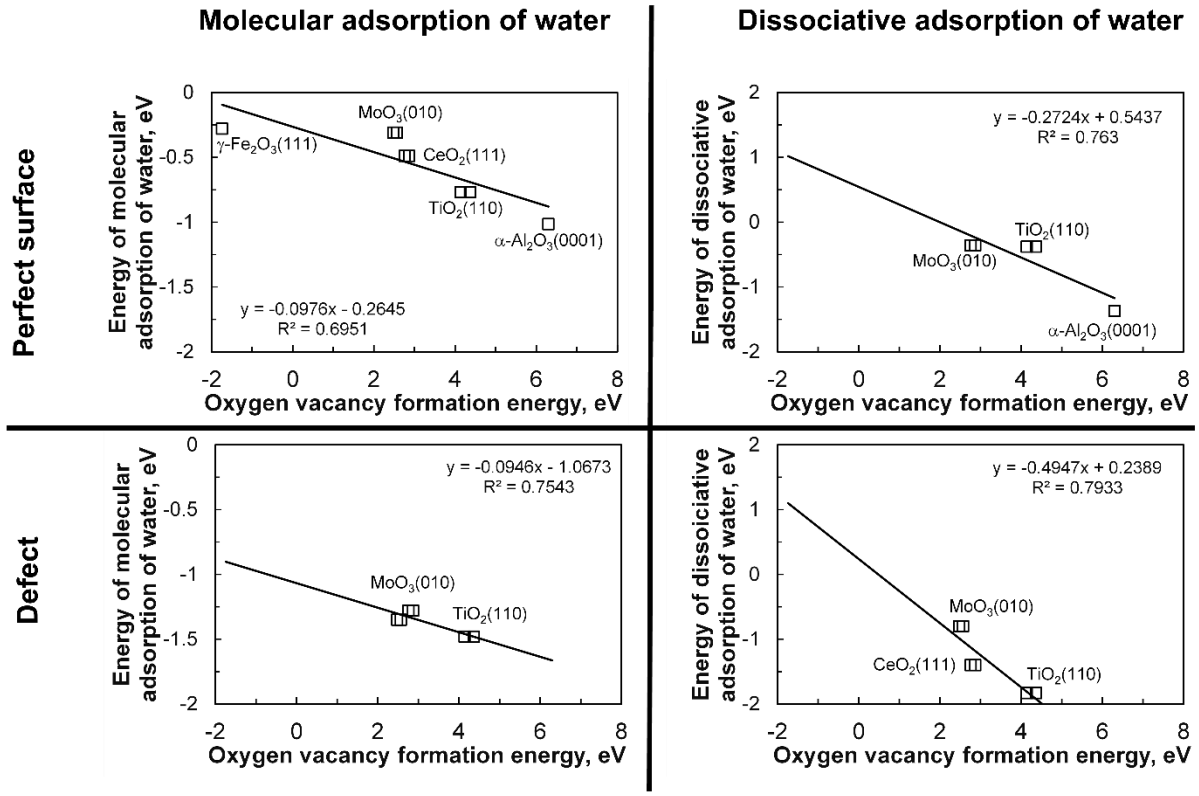

Figure S7. Correlating the energy of adsorption of water on perfect surfaces and defect sites[S17-S20] with the oxygen vacancy formation.[S13-S16]

References

1. Galet, L.; Patry, S.; Dodds, J. *J. Colloid Interface Sci.* **2010**, *346*, 470–475. https://doi.org/10.1016/j.jcis.2010.02.051.
2. Taguta, J.; O'Connor, C.T.; McFadzean, B. *Colloids Surfaces A Physicochem. Eng. Asp.* **2018**, *558*, 263–270. https://doi.org/10.1016/j.colsurfa.2018.08.059.
3. Neirinck, B.; Van Deursen, J.; Van der Biest, O.; Vleugels, *J. Amer. Cer. Soc.* **2010**, *93*, 2515-2518. https://doi.org/10.1111/j.1551-2916.2010.03854.x.
4. Alheshibri, M.; Albetran, H.M.; Abdelrahman, B.H.; Al-Yaseri, A.; Yekeen, N.; Low, I.M. *Materials* **2022**, *15*, 5485. https://doi.org/10.3390/ma15165485.
5. Kong, X.; Hu, Y.; Wang, X.; Pan, W. *J. Adv. Ceram.* **2016**, *5*, 284–290. https://doi.org/10.1007/s40145-016-0201-5.
6. Fronzi, M.; Assadi, M.H.N. ; Hanaor, D.A.H. *Appl. Surf. Sci.* **2019**, *478*, 68–74. https://doi.org/10.1016/j.apsusc.2019.01.208.
7. Sreelakshmi, V.R.; Anu Kaliani, A.; Jithin, M. *J. Mater. Sci.: Mater. Electron.* **2022**, *33*, 9525–9537. https://doi.org/10.1007/s10854-021-07504-y.
8. Bazhan, Z.; Ghodsi, F.E.; Mazloom, J. *J. Mater. Sci.: Mater. Electron.* **2018**, *29*, 11489–11497. https://doi.org/10.1007/s10854-018-9244-4.
9. Morimoto, T.; Shiomi, K.; Tanaka, H. *Bull. Chem. Soc. Jap.* **1964**, *37*, 392-395. https://doi.org/10.1246/bcsj.37.392.
10. Morimoto, T.; Nagao, M.; Omori, T. *Bull. Chem. Soc. Jap.* **1969**, *42*, 943-946. https://doi.org/10.1246/bcsj.42.943.
11. Haruo, W.; Jun'etsu, S. *Bull. Chem. Soc. Jap.* **1988**, *61*, 3067-3072. https://doi.org/10.1246/bcsj.61.3067.
12. Pustovarov, V.A.; Perevalov, T.V.; Gritsenko, V.A.; Smirnova, T.P.; Yelisseyev, A.P. *Thin Solid Films* **2011**, *519*, 6319-6322. https://doi.org/10.1016/j.tsf.2011.04.014.
13. Hinuma, Y.; Toyao, T. ; Kamachi, T. ; Maeno, Z. ; Takakusagi, S.; Furukawa, S. ; Takigawa, I.; Shimizu, K.-i. *J. Phys. Chem. C* **2018**, *122*, 29435–29444. https://doi.org/10.1021/acs.jpcc.8b11279.
14. Li, H. ; Guo, Y. ; Robertson, J. *J. Phys. Chem. C* **2015**, 119, 18160–18166. https://doi.org/10.1021/acs.jpcc.5b02430.
15. Mayernick, A.D. ; Janik, M.J. *J. Phys. Chem. C* **2008**, *112*, 14955–14964. https://doi.org/10.1021/jp805134s.
16. Jian, W.; Wang, S.-P.; Zhang, H.-X.; Bai, F.-Q. *Inorg. Chem. Front.* **2019**, *6*, 2660-2666. https://doi.org/10.1039/C9QI00351G.
17. Hass, K.C.; Schneider, W.F.; Curioni, A.; Andreoni, W. *J. Phys. Chem. B* **2000**, *104*, 5527–5540. https://doi.org/10.1021/jp000040p.
18. Martinez-Casado, R.; Mallia, G.; Harrison, N.M.; Pérez, R. *J. Phys. Chem. C* **2018**, *122*, 20736-20744. https://doi.org/10.1021/acs.jpcc.8b05081.

19. Fronzi, M.; Piccinin, S.; Delley, B.; Traversa, E.; Stampfl, C. *Phys. Chem. Chem. Phys.* **2009**, *11*, 9188–9199. https://doi.org/10.1039/B901831J.
20. Head, A.R.; Gattinoni, C.; Trotochaud, L.; Yu, Y.; Karslıoğlu, O.; Pletincx, S.; Eichhorn, B.; Bluhm, H. *J. Phys. Chem. C* **2019**, *123*, 16836–16842. https://doi.org/10.1021/acs.jpcc.9b03822.
21. Ntallis, N.; Peyre, V.; Perzynski, R.; Dubois, E.; Trohidou, K.N. *J. Magn. Magn. Mater.* **2019**, *484*, 74–82. https://doi.org/10.1016/j.jmmm.2019.03.132.
22. Tilocca, A.; Selloni, A. *J. Phys. Chem. B* **2004**, *108*, 4743–4751. https://doi.org/10.1021/jp037685k.

